X SEPOPE

21 a 25 de maio de 2006

May – 21rst to 25th – 2006
FLORIANÓPOLIS (SC) – BRASIL

X SIMPÓSIO DE ESPECIALISTAS EM PLANEJAMENTO DA OPERAÇÃO E EXPANSÃO ELÉTRICA

X SYMPOSIUM OF SPECIALISTS IN ELECTRIC OPERATIONAL AND EXPANSION PLANNING

Simulation of Power Systems Dynamics using Dynamic Phasor Models

Turhan Demiray

Email: demirayt@eeh.ee.ethz.ch

Göran Andersson

Email: andersson@eeh.ee.ethz.ch

Power Systems Laboratory

ETH Zürich – Switzerland

SUMMARY

Dynamic phasor modeling technique is mostly applied on power electronics devices. In this paper, application of the dynamic phasor modeling technique is extended to other major power system components. Starting from the detailed time-domain models, the dynamic phasor models for these components are derived and implemented. Further, an efficiency and accuracy comparison of the dynamic phasor modeling technique with other conventional modeling techniques - like the standard models in three-phase ABC reference frame (e.g. in EMTP) and models in DQ0 reference frame (e.g. in SIMPOW) - is given. A systematic comparison is warranted by simulating these differently modeled components in a Matlab based common simulation framework. Furthermore reduced order dynamic phasor models of the components are derived and results are compared with other production-grade transient stability programs. Simulation results for two test cases are shown.

KEYWORDS

Dynamic Phasors, Transient Stability, Hybrid Systems

1. Introduction

The dynamic behavior and stability of power systems are most often studied with the so called transient stability programs. Traditionally in most of these programs the phasor model approach is used. Recent developments, particularly the introduction of more power electronics based equipment e.g. HVDC and FACTS components, show that there is a shortage in the analysis methods with fundamental frequency phasor models. For such components a full time domain simulation might be needed. Due to the limitation of computer storage and computation time, a complete representation of a large power system in an electromagnetic transients program is very difficult and won't give additional information. To overcome this problem, the concept of time-varying Dynamic phasors is proposed [1] to model power electronics based equipment similar approaches have been reported in [2]. It has several advantages over phasor based methods. Firstly, it has a wider bandwidth in the frequency domain than the quasi-stationary phasor. Secondly, dynamic phasors can be used to compute fast electromagnetic transients with larger time steps, so that it drastically reduces the simulation time compared with conventional time domain EMTP like simulation. *Phasor Dynamics Approach* provides a middle ground between the approximations inherent in a phasor based *sinusoidal quasi-steady-state* representation, and the analytic complexity and computational burden associated with representing network voltages and currents in time-domain.

Section 2 gives a brief overview of the different modeling techniques, which are commonly used in production-grade programs for modeling of power system components. It further contains an introduction to the concept of time-varying Fourier coefficients, which is used as an analytical tool for deriving dynamic phasor models. Section 3 focuses on the structural overview of the used simulation framework and implemented tools such as *Automatic Code Generator* and *Dynamic Phasor Model Generator*, which are used in this work to automate the source code creation of component models. Section 4 comprises the implemented models and used test cases. And finally section 5 gives a comparison of simulation results.

2. Different Modeling Techniques

2.1. Models in Three-Phase (ABC) Reference Frame

True “physical” models in three-phase reference frame are the starting point for the modeling techniques which will be treated in the following sections. All electrical quantities of the electrical network such as voltages, currents etc. and all model equations are given in the three-phase (ABC) reference frame. Such models are commonly used in EMTP like detailed time-domain simulation programs. In ABC reference frame any kind of equipment can be modeled easily e.g. power electronic based equipments such as FACTS and HVDC. But the efficiency of the simulation can suffer from the periodicity due to the presence of AC phase quantities (50, 60 Hz) even during steady state conditions.

2.2. Models in DQ0 Reference Frame

The DQ0 reference frame is an “at the system frequency rotating” reference frame, which is commonly used in the derivation of synchronous machine equations as described in [3]. One of the advantages in analyzing the synchronous machine equations in DQ0 reference frame is that under balanced steady-state operation stator quantities have constant values and for other modes of operation this quantities vary slowly with time (2-3 Hz). This advantage leads also to faster simulation times under balanced conditions, as the variation of variables in DQ0 reference frame are much slower than the original variables in three-phase ABC reference frame. Therefore in some programs (e.g. SIMPOW [4]) the DQ0 transformation is applied to all components in the system. All variables and equations of the models in three-phase ABC reference frame are transformed to DQ0 reference frame. The DQ0 transformation is a single reference frame transformation as the reference frame rotates with system frequency. Therefore the simulations in DQ0 reference frame will be efficient around system frequency. But if there are unbalanced conditions in the system or other harmonics, this efficiency can

decrease drastically. Mathematically, the DQ0 or Park's transformation is given by the following equation in (2.1), where $\theta = \omega_s t = 2\pi f_s t$ and f_s is the system frequency.

$$(2.1) \qquad \begin{bmatrix} i_d(t) \\ i_q(t) \\ i_0(t) \end{bmatrix} = \frac{2}{3} \begin{bmatrix} \cos(\theta) & \cos(\theta - \frac{2\pi}{3}) & \cos(\theta + \frac{2\pi}{3}) \\ \sin(\theta) & \sin(\theta - \frac{2\pi}{3}) & \sin(\theta + \frac{2\pi}{3}) \\ \frac{1}{2} & \frac{1}{2} & \frac{1}{2} \end{bmatrix} \cdot \begin{bmatrix} i_a(t) \\ i_b(t) \\ i_c(t) \end{bmatrix} \Rightarrow i_{dq0}(t) = T_{dq0} \cdot i_{abc}(t)$$

Here we used the phase current as an example of a phase quantity. The inverse transformation is given by $i_{abc}(t) = T_{abc} \cdot i_{dq0}(t)$ with $T_{abc} = T_{dq0}{}^{-1}$. The derivatives of the ABC phase quantities can be written as

$$(2.2) \qquad \frac{di_{abc}}{dt} = \frac{di_{dq0}}{dt} + \begin{bmatrix} 0 & \omega_s & 0 \\ -\omega_s & 0 & 0 \\ 0 & 0 & 0 \end{bmatrix} \cdot i_{dq0} \Rightarrow \frac{di_{dq0}}{dt} + J \cdot i_{dq0}.$$

2.3. Dynamic Phasor Models

If power electronics based equipments are used in the power system, the assumption of only having frequencies near to the fundamental frequency is usually not valid any more as shown in Figure 1. For example in the case of TCSC - depending on the conduction angle - other harmonics have a significant participation in the transient waveforms of voltage and current.

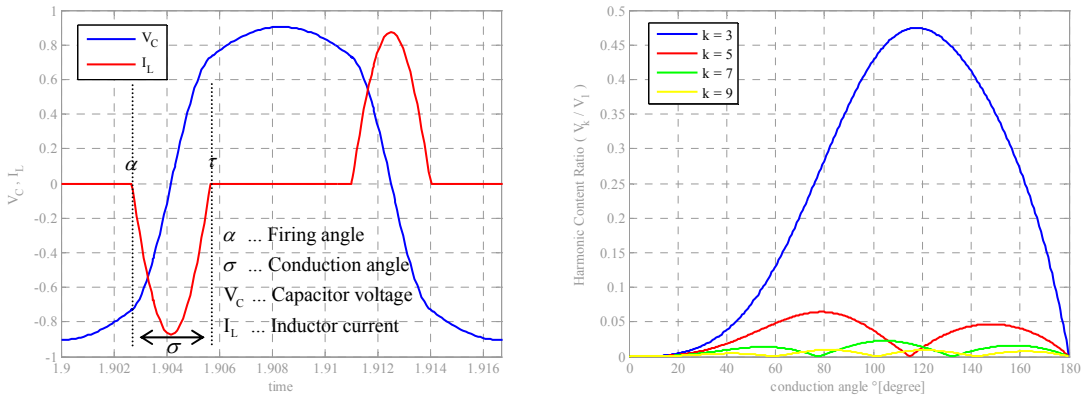

Figure 1: TCSC: Transient waveforms and Harmonic content ratio as a function of the conduction angle

The main idea behind dynamic phasor modeling is to approximate a real valued periodic waveform $x(\tau)$ in the interval $\tau \in (t-T, t]$ with a Fourier series form [5]

$$(2.3) \qquad x(\tau) = \sum_{k=0}^{\infty} X_{k,c}(t)\cos(k\omega_s\tau) + X_{k,s}(t)\sin(k\omega_s\tau)$$

where, $\omega_s = 2\pi/T$ and $X_{k,c}(t)$ and $X_{k,s}(t)$ are the time-varying Fourier coefficients. $X_{k,c}(t)$ and $X_{k,s}(t)$ can be determined by the following averaging operations.

$$(2.4) \qquad \begin{aligned} X_{k,c}(t) &= \frac{1}{T}\int_{t-T}^{t} x(\tau)\cdot\cos(k\omega_s\tau)\cdot d\tau = \langle x \rangle_{k,c}(t) \\ X_{k,s}(t) &= \frac{1}{T}\int_{t-T}^{t} x(\tau)\cdot\sin(k\omega_s\tau)\cdot d\tau = \langle x \rangle_{k,s}(t) \end{aligned}$$

A key factor in developing dynamic phasor models is the relation between the derivatives of $x(\tau)$ and the derivatives of $X_{k,c}(t)$ and $X_{k,s}(t)$, which is given in (2.5). Another important property is that the product of two time-domain variables equals a discrete time convolution of the two dynamic phasor sets of the variables.

$$\left\langle \frac{dx}{dt} \right\rangle_{k,c} = \frac{dX_{1,c}}{dt} - k \cdot \omega_s \cdot X_{1,s}$$
$$\left\langle \frac{dx}{dt} \right\rangle_{k,s} = \frac{dX_{1,s}}{dt} + k \cdot \omega_s \cdot X_{1,c} \tag{2.5}$$

3. Simulation Framework

To be able to make a systematic comparison between the efficiency and accuracy of the mentioned modeling techniques, we have implemented all the major components of a power system (Synchronous machines, Transformers, Lines, Loads, TCSC etc.) in a common simulation framework where all equations of the power system are solved simultaneously. In this chapter, a structural overview of the implemented simulation framework is given.

3.1. Hybrid System Representation

Power systems are an important class of *hybrid systems* as they exhibit interactions between continuous dynamics and discrete events [6],[7]. Components of such hybrid systems can be modelled by a set of Differential, Switched Algebraic and State-Reset (DSAR) equations (3.1)

$$\begin{aligned}
&\dot{\underline{x}} = \underline{f}(\underline{x}, y) \\
&0 = g^{(0)}(\underline{x}, y) \\
&0 = \begin{cases} g^{(i^-)}(\underline{x}, y) & y_{d,i} < 0 \\ g^{(i^+)}(\underline{x}, y) & y_{d,i} > 0 \end{cases} \qquad i = 1,\ldots\ldots,d \qquad \underline{x} = \begin{bmatrix} x \\ z \\ \lambda \end{bmatrix}, \underline{f} = \begin{bmatrix} f \\ 0 \\ 0 \end{bmatrix}, \underline{h}_j = \begin{bmatrix} x \\ h_j \\ \lambda \end{bmatrix} \\
&\underline{x}^+ = \underline{h}(\underline{x}^-, y^-) \qquad y_{e,j} = 0 \qquad j \in \{1,\ldots\ldots,e\}
\end{aligned} \tag{3.1}$$

where

- x are continuous dynamic states,
- z are discrete states,
- y are algebraic states, y_d and y_e are so called *event* variables which trigger events if they change sign (y_d) and/or pass through zero (y_e),
- λ are parameters.

The overall system is built by connecting the *interface* variables of the components together. These connections can be formulated by simple algebraic equations ($y_{1,1} = y_{3,4} \Rightarrow c(y) = y_{1,1} - y_{3,4} = 0$).

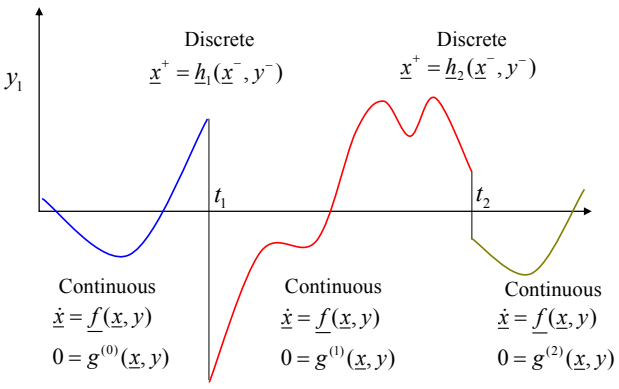

Figure 2: Simulation Flow - Differential, Switched Algebraic and State-Reset (DSAR) equations

As shown in Figure 2, between events the system behavior is governed by the differential algebraic equations $\dot{\underline{x}} = \underline{f}(\underline{x}, y)$ and $g^{(i)}(\underline{x}, y) = 0$. At time $t = t_1$ an event occurs and the corresponding post-event values of discrete and continuous dynamic states x^+ are calculated according to $\underline{x}^+ = \underline{h}(\underline{x}^-, y^-)$, where superscript $^+$ means post-event values and $^-$ means pre-event values of the corresponding variable. After x^+ are calculated, post-event values of algebraic variables y^+ are calculated by solving the nonlinear equation $g^{(1)}(\underline{x}^+, y^+) = 0$ at $t = t_1$. After post-event values x^+ and y^+ are determined, they serve as initial conditions for the new continuous section. The system behavior in this section is governed by the equations $\dot{\underline{x}} = \underline{f}(\underline{x}, y)$ and $g^{(1)}(\underline{x}, y) = 0$. The overall system equations are given by (3.2), where in this formulation x, y contain all model variables and f, g all model equations. The connection equations $c(y)$ can be included in $g(\underline{x}, y) = 0$.

$$(3.2) \qquad \begin{matrix} \dot{\underline{x}} = \underline{f}(\underline{x}, y) \\ 0 = g(\underline{x}, y) \\ 0 = c(y) \end{matrix} \Rightarrow \begin{Bmatrix} \underline{x}_{n+1} = \underline{\Psi}\ (h, f(\underline{x}_{n+1}, y_{n+1}), f(\underline{x}_n, y_n)...) \\ 0 = g(\underline{x}_{n+1}, y_{n+1}) \\ 0 = c(y_{n+1}) \end{Bmatrix} \Rightarrow F(\underline{x}_{n+1}, y_{n+1}) = 0$$

If we discretize the differential equations with an implicit integration method $\underline{x}_{n+1} = \underline{\Psi}\ (h, f(\underline{x}_{n+1}, y_{n+1}), f(\underline{x}_n, y_n)...)$, we end up in a nonlinear set of implicit algebraic equations $F(\underline{x}_{n+1}, y_{n+1}) = F(\chi) = 0$ with $\chi = [\underline{x}_{n+1}, y_{n+1}]$. This equation can be solved iteratively according to $\chi_{i+1} = \chi_i - F_\chi^{-1}(\chi_i) \cdot F(\chi_i)$ where $F_\chi(\chi)$ is the Jacobian of $F(\chi)$ with respect to χ (3.3).

$$(3.3) \quad F(\chi) = \begin{pmatrix} \Psi(h, f(\underline{x}_{n+1}, y_{n+1}), f(\underline{x}_n, y_n), ...) - \underline{x}_{n+1} \\ g(\underline{x}_{n+1}, y_{n+1}) \\ c(y_{n+1}) \end{pmatrix}, \; F_\chi(\chi) = \begin{bmatrix} \left(\Psi_f \cdot f_x - I\right) & \left(\Psi_f \cdot f_y\right) \\ g_x & g_y \\ 0 & c_y \end{bmatrix}.$$

From (3.3) we can see, that the simulation kernel needs the evaluation of f, g and the partial derivatives f_x, f_y, g_x, g_y from every model to solve the nonlinear algebraic equation set $F(\chi) = 0$. Ψ, Ψ_f are dependent on the applied numerical integration method and c, c_y are dependent on the connections. Because of its numerical stability, the Trapezoidal Integration Method with variable step control is used as numerical integration method in this framework.

3.2. Automatic Code Generator

The simulation kernel is implemented in Matlab and the models are specified in so called *Model Definition File (**MDF**)*, where the user simply defines the equations and variables of the model as they are given in (3.1). As proposed in [7] we have also implemented an *Automatic Code Generator (**ACG**)* in Matlab. ACG takes the MDF and creates the Matlab code for the model using the Symbolic Differentiation facility in Matlab for the analytical calculation of f_x, f_y, g_x, g_y.

All models of the major power system components are implemented in ABC and DQ0 reference frame in this framework. To automate the creation of the dynamic phasor models from their ABC or DQ0 models, we built in an interface called *Dynamic Phasor Model Generator*. It takes the MDF of the model in ABC or DQ0 form. Using (2.3) and (2.5) the continuous dynamic states and algebraic states are replaced with the approximated counterparts in the model equations (3.1) which leads to

$$f(x, y) \Rightarrow f(X_0, X_{1c} \cdot \cos(\omega_s t), X_{1s} \cdot \sin(\omega_s t), ..., Y_0, Y_{1c} \cdot \cos(\omega_s t), Y_{1s} \cdot \sin(\omega_s t) .....)$$
$$g(x, y) \Rightarrow g(X_0, X_{1c} \cdot \cos(\omega_s t), X_{1s} \cdot \sin(\omega_s t), ..., Y_0, Y_{1c} \cdot \cos(\omega_s t), Y_{1s} \cdot \sin(\omega_s t) .....)$$

By using (2.4) we can transform the set of f, g equations of the model into a new set of equations and get the definition of the phasor dynamic model in a new set of functions (3.4),

$$(3.4)\qquad \begin{aligned} \dot{x} &= f(x,y) \\ 0 &= g(x,y) \end{aligned} \quad \Rightarrow \quad \begin{aligned} \dot{X}_{k,c} &= F_{k,c}(X_{k,c}, X_{k,s}, Y_{kc}, Y_{ks}) - k \cdot \omega_s \cdot X_{k,s} \\ \dot{X}_{k,s} &= F_{k,s}(X_{k,c}, X_{k,s}, Y_{kc}, Y_{ks}) + k \cdot \omega_s \cdot X_{k,c} \\ 0 &= G_{k,c}(X_{k,c}, X_{k,s}, Y_{kc}, Y_{ks}) \\ 0 &= G_{k,s}(X_{k,c}, X_{k,s}, Y_{kc}, Y_{ks}) \end{aligned}$$

where k is set of phasors which are used for the approximation in (2.3) [e.g. $k = \{0,1,2\}$]. Figure 3 shows the schematic view of the Automatic Code Generation.

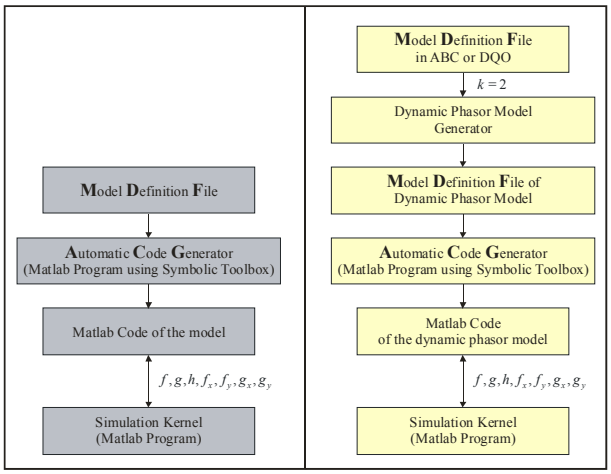

Figure 3

4. Models and Test systems

We implemented the **synchronous machine** model in DQ0 reference frame as described in [3 , p. 86]. Starting from this model we derived then the dynamic phasor model of the synchronous machine by choosing k={0,1,2} in (3.4). The reason for this is to include positive (k=0), zero (k=1), negative (k=2) sequence quantities [8] to simulate also unbalanced conditions in our model. We used the standard Π model for **transmission lines** and parallel RLC model for **loads**. But other models can also be implemented easily.

The implemented **TCSC** model is based on the work described in [1]. The time domain equations for TCSC are given in (4.1), where $q = 1$ if one of the thyristors is conducting and $q = 0$ if both thyristors are blocking. The main idea here is to approximate the capacitor voltage by $v(t) \approx \sum_k V_{k,c} \cdot \cos(\omega_s t) + V_{k,s} \cdot \sin(\omega_s t)$ with $k = 1,3,5$, to include the participations of major harmonics as illustrated in Figure 1. As a second step a steady-state approximation is applied on $V_{k,c}$ and $V_{k,s}$ for $k = 3,5$ with $V_{k,c} = f\left(V_{1c}, V_{1s}, \rho_k(\sigma)\right)$ and $V_{k,s} = f\left(V_{1c}, V_{1s}, \rho_k(\sigma)\right)$, where $\rho_k(\sigma)$ is the steady-state harmonic content ratio as a function of the conduction angle.

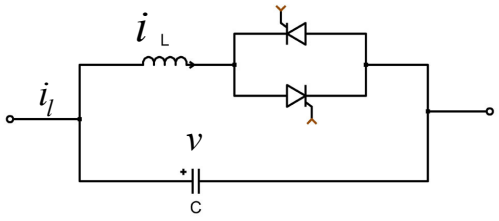

$$(4.1)\qquad \begin{aligned} C\frac{dv}{dt} &= i_l - i \\ L\frac{di}{dt} &= q \cdot v \end{aligned} \quad \Rightarrow \quad \begin{aligned} C\frac{dV_{1c}}{dt} &= I_{l,1c} - I_{1c} - \omega_s V_{1s} \\ L\frac{dI_{1c}}{dt} &= f_{1c}\left(V_{1c}, V_{1s}, \rho_3(\sigma), \rho_5(\sigma)\right) \end{aligned} \quad \text{and} \quad \begin{aligned} C\frac{dV_{1s}}{dt} &= I_{l,1s} - I_{1s} + \omega_s V_{1c} \\ L\frac{dI_{1s}}{dt} &= f_{1s}\left(V_{1c}, V_{1s}, \rho_3(\sigma), \rho_5(\sigma)\right) \end{aligned}$$

SMIB (Single Machine Infinite Bus) and Two Area system are used as test systems with the data given in [3].

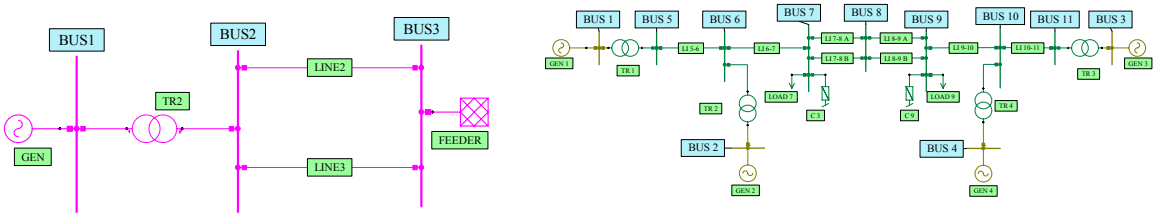

Figure 4: Single line diagram of SMIB and Two Area System

5. Simulation Results

As mentioned in section 4 all dynamic phasor models of the components are derived from DQ0 models with k = {0,1,2}. But a derivation from ABC models is also possible.

5.1. Simulations with Detailed Time Domain Models

In both test systems, a one-phase to ground fault is applied as a disturbance at 0.1 s and removed at 0.17 s. In Figure 5 and Figure 6 the electrical torque of the synchronous machines "GEN" (SMIB) and "GEN1" (Two Area system) are shown. In both figures we have the overall simulation interval and a zoomed section during the unbalanced condition. For verification of our results, SMIB system has also been implemented in PLECS [9] and simulation results are compared with those in our framework. PLECS is a toolbox for high-speed simulations of electrical and power electronic circuits under MATLAB/Simulink. We see a very good overall agreement between all results, especially in the zoomed sections. In the table 1, the computation times for these simulations are compared. The simulations in DQ0 reference frame are the fastest. In these two test cases, the unbalanced conditions only last for 0.07 s, all implemented components are symmetrical components and no power electronic devices are used. As stated in section 2.2, under balanced conditions and with frequencies near to the fundamental (system) frequency, the choice of DQ0 reference frame is the best choice for efficient computation. But if the computation times during the unbalanced conditions are compared, the simulations with dynamic phasor models with k={0,1,2} are more efficient. The reason for this is, during unbalanced conditions zero and negative sequence quantities appear as system inherent "harmonics" in DQ0 reference frame (zero sequence→50Hz and negative sequence →100Hz). The time step size during simulation must be kept small enough to simulate these oscillations. But if dynamic phasor models are used, these mentioned system inherent harmonics are already included in the model equations with k=1 (zero sequence) and k=2 (negative sequence), and simulation time is marginally influenced.

	ABC	DQ0	k= (0,1,2)
SMIB	121 sec	20 sec	32 sec
Two Area System	453 sec	272 sec	350 sec

Table 1

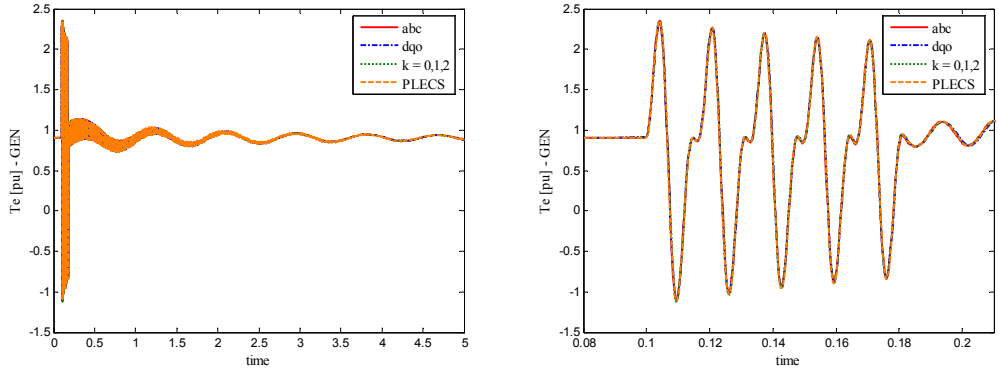

Figure 5: SMIB – One phase to ground fault at BUS2 at 0.1s and cleared at 0.17s

The dynamic phasor approach is a projection of a signal on a multiple-orthogonal reference frame (2.4), where time signals $\cos(k\omega_s t)$ and $sin(k\omega_s t)$ are orthogonal base signals (vectors).

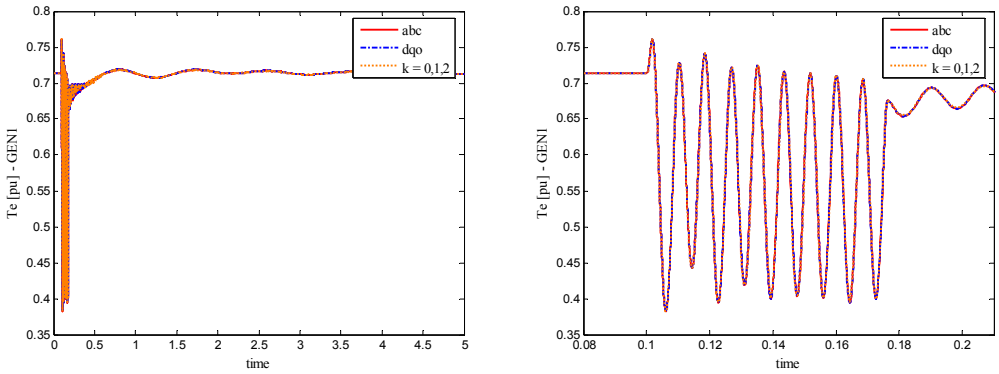

Figure 6: Two Area System – One phase to ground fault at BUS8 at 0.1 and cleared at 0.17

5.2. Simulations with dynamic phasor TCSC model

To test the implemented TCSC model described in section 4, we modified the Two Area System in Figure 4. We have split BUS8 into BUS8 and BUS12 and placed the TCSC between these nodes. In our simulation the firing angle of the thyristors are changed from 68.3° to 59° at 0.2 s and back again at 0.5 s. Achieved results are given in Figure 7. The simulation time with ABC models was about 230 s and with the phasor dynamic models about 20 s.

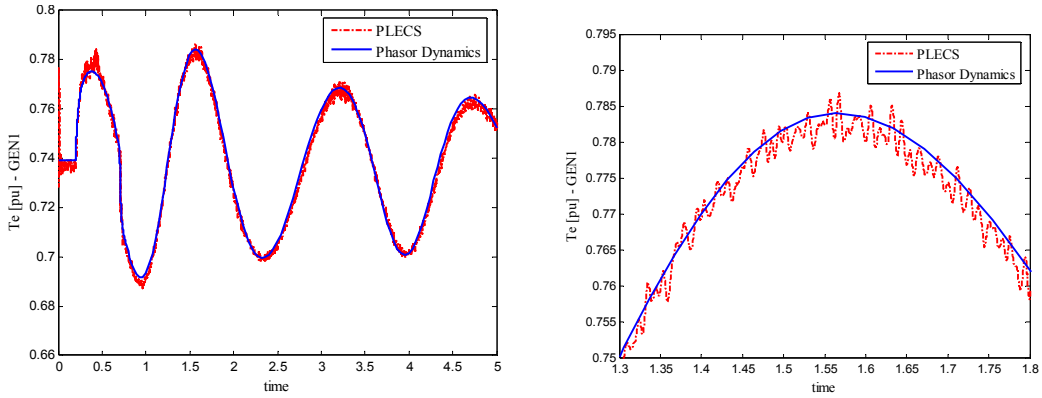

Figure 7: Two Area System – Changing of firing angle from 68.3° to 59° at 0.2 s and back again at 0.5 s

5.3. Simulations with Reduced Order Models

As next step, we made an eigenanalysis and a time-scale decomposition to reduce the order of the dynamic phasor models. We looked at the eigenvalues and their participation factors. Dynamics of continuous states with very low participation in the slow modes has been neglected, which means for those states the $\dot{X}_{k,c}$ and $\dot{X}_{k,s}$ are set to zero in equation (3.4). Same approach has also been applied on the DQ0 reference frame models, which leads to fundamental frequency models used in transient stability programs. We used same test system (SMIB) and the same faults. The simulation results with reduced order models are compared with those in NEPLAN and SIMPOW [4, 10] in Figure 8. The left part of the figure shows the positive-sequence electrical torque, where the dotted curve labeled "PLECS" is calculated from the actual time domain signal by setting k=0 in equation (2.4). The right part of the figure shows the negative sequence electrical torque during unbalanced conditions, where again the dotted curves labeled "PLECS" are calculated from the actual time domain signal by setting k=2 in equation (2.4). Even though we are using reduced order models, the results show an overall agreement. Usually in transient stability programs the negative and zero sequence networks are not simulated directly, but their effects in the positive-sequence network are taken into account by appropriately combining the equivalent negative and zero sequence impedances depending on the

fault-type as described in [3]. With the use of phasor dynamic models with k = {0,1,2}, it was also possible to simulate the zero and negative sequence quantities throughout in the system during unbalanced conditions in a systematic way. The simulation time with detailed models was 128 s and with reduced order phasor dynamic models 9 s.

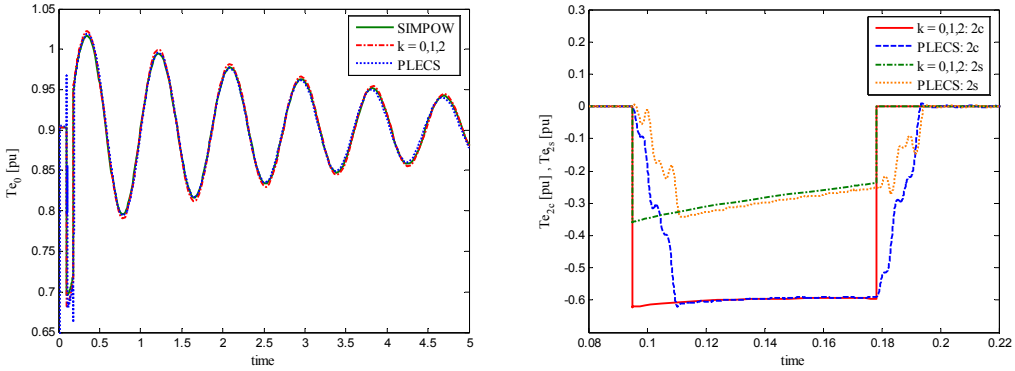

Figure 8: SMIB – One phase to ground fault at BUS2 at 0.1 and cleared at 0.17

6. Conclusions

In this paper we have applied the phasor dynamics approach to major power system components and compared the accuracy and efficiency with different modeling techniques such as models in ABC and DQ0 reference frame. Simulations with ABC reference frame models are accurate but not so efficient. On the other hand, simulations with DQ0 reference frame models are accurate and also efficient under balanced conditions and with frequencies near to the fundamental (system) frequency. If we have unbalanced conditions or other frequencies (harmonics) in the system than the fundamental frequency (e.g. usage of power electronic based equipment), a single reference transformation like DQ0 transformation becomes inefficient for simulation. In such cases phasor dynamic models show a better performance because of their multi reference frame characteristics, but here the accuracy depends on the appropriate selection of the set of k in equation (2.3).

ACKNOWLEDMENT

The authors would like to thank BCP for their financial support, Dr. Luigi Busarello and Giatgen Cott for stimulating discussions and Ian A. Hiskens & Marek Zima for making the source codes of their files available. These files have been very useful information while implementing this simulation framework.

BIBLIOGRAPHY

[1] P. Mattavelli, G. C. Verghese, and A. M. Stankovic, "Phasor dynamics of thyristor-controlled series capacitor systems," *Power Systems, IEEE Transactions on*, vol. 12, pp. 1259-1267, 1997.

[2] W. Hammer and G. Andersson, "Dynamic Modeling of Capacitor Commutated Converters," invited paper 004, SEPOPE IX, Rio de Janeiro, Brazil, 2004.

[3] P. Kundur, N. J. Balu, and M. G. Lauby, *Power system stability and control*. New York: McGraw-Hill, 1994.

[4] STRI, "Power System Simulation & Analysis Software SIMPOW, User Manual, http://www.stri.se."

[5] S. R. Sanders, J. M. Noworolski, X. Z. Liu, and G. C. Verghese, "Generalized averaging method for power conversion circuits," *Power Electronics, IEEE Transactions on*, vol. 6, pp. 251-259, 1991.

[6] I. A. Hiskens and M. A. Pai, "Hybrid systems view of power system modelling," presented at Circuits and Systems, 2000. Proceedings. ISCAS 2000 Geneva. The 2000 IEEE International Symposium on, 2000.

[7] I. A. Hiskens and P. J. Sokolowski, "Systematic modeling and symbolically assisted simulation of power systems," *Power Systems, IEEE Transactions on*, vol. 16, pp. 229-234, 2001.

[8] A. M. Stankovic and T. Aydin, "Analysis of asymmetrical faults in power systems using dynamic phasors," *Power Systems, IEEE Transactions on*, vol. 15, pp. 1062-1068, 2000.

[9] Plexim, "PLECS User Manual - High-speed simulations of electrical and power electronic circuits under MATLAB/Simulink."

[10] BCP, "NEPLAN software manual, http:\\www.neplan.ch."